

A high precision shear deformable element for free vibration of thick/thin composite trapezoidal plates

S. Haldar[†] and M. C. Manna[‡]

Department of Applied Mechanics, B. E. College (D. U.), Howrah-7111 03, India

(Received December 16, 2002, Revised May 19, 2003, Accepted June 5, 2003)

Abstract. A high precision shear deformable triangular element has been proposed for free vibration analysis of composite trapezoidal plates. The element has twelve nodes at the three sides and four nodes inside the element. Initially the element has fifty-five degrees of freedom, which has been reduced to forty-eight by eliminating the degrees of freedom of the internal nodes through static condensation. Plates having different side ratios (b/a), boundary conditions, thickness ratios ($h/a=0.01, 0.1$ and 0.2), number of layers and fibre angle orientations have been analyzed by the proposed shear locking free element. Trapezoidal laminate with concentrated mass at the centre has also been analyzed. An efficient mass lumping scheme has been recommended, where the effect of rotary inertia has been included. For validation of the present element and formulation few results of isotropic trapezoidal plate and square composite laminate have been compared with those obtained from open literatures. The numerical results for composite trapezoidal laminate have been given as new results.

key words: finite element; shear-locking free element; composite trapezoidal plate; rotary inertia; first order shear deformation theory; lump mass.

1. Introduction

The finite element method (Zienkiewicz and Taylor 1988) is regarded as the most versatile analysis tool specifically in structural analysis problems. The plate bending is one of the first problems where finite element was applied in early sixties. The initial attempts were made with thin plates based on Kirchhoff's hypothesis where a number of difficulties were encountered. These are mostly concerned with the satisfaction of normal slope continuity along the element edges. Subsequently, the method has been applied to thick plates based on Reissner-Mindlins hypothesis where the above problem has been avoided by considering the transverse displacement (w) and rotations of normal (θ_x and θ_y) as independent displacement components. Amongst the thick plate elements developed so far, the most prominent elements are the isoparametric elements, which became very popular. Though these elements are quite elegant, they involve certain problems such as shear locking, stress extrapolation, spurious modes etc. Keeping these aspects in view some research workers have tried to develop an element, which will be free from the above problems. The necessity has been geared up further with the wide use of fibre reinforced laminated composite which is weak in shear due to its low shear modulus compared to elastic modulus. As an outcome of these facts, some elements have been proposed by

[†]Lecturer: salihaldar@lycos.com

[‡]Lecturer

Petrolito (1989), Yuan and Miller (1989), Sengupta (1991), Batoz and Katili (1992), Zhongnian (1992), Wanji and Cheung (2000) and a few others.

Exact thin plate solutions for isotropic trapezoidal plates are available only for certain boundary conditions (Timoshenko and Woinowsky-Krieger 1959). For complex boundary conditions a numerical method must therefore be used. Plates of arbitrary shaped subjected to static load was analysed by Liew (1992) using the principle of minimum potential energy with admissible $pb-2$ Ritz functions. A majority of the arbitrarily shaped plate problems in bending was solved numerically by finite element method (Gallagher 1975 and Zienkiewicz 1971). Free flexural vibration of multi-layered symmetric and unsymmetric composite laminates with symmetric trapezoidal planform of arbitrary combination of edge conditions was investigated by Liew and Lim (1995). Lim *et al.* (1996) studied the free vibration of general thin composite trapezoidal plates using Ritz extremum energy principle with kinematically oriented $pb-2$ shape function. Liew *et al.* (1999) analysed free flexural vibration of arbitrary quadrilateral unsymmetrically laminated plates subjected to arbitrary boundary conditions using Ritz procedures.

In the present work a high precision composite shear deformation element has been proposed. The element has the advantage that plates of any shapes can be modelled by this element, as it has a triangular geometry. In this element a fourth order complete polynomial has been used to express transverse displacement w while the in-plane displacements (u and v) and the rotations of the normal (θ_x and θ_y) have been expressed with complete cubic polynomials. Thus the interpolation function of w is one order higher than those of θ_x and θ_y , which has helped to make this element free from locking in shear and other relevant problems.

2. Formulation

The formulation is based on Mindlin’s plate theory, which ensures the incorporation of shear deformation effects. The middle plane of the plate has been considered as the reference plane.

A typical element shown in Fig. 1 has sixteen nodes. The locations of the nodes 3, 7 and 11 are at the midpoint of the corresponding sides while nodes 2, 4, 6, 8, 10 and 12 are located at a distance of one

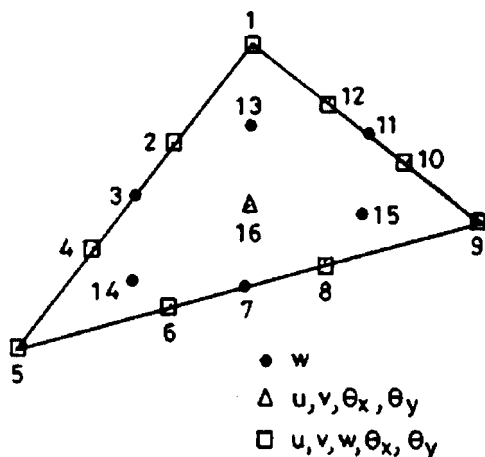


Fig. 1 A typical element with nodes and degrees of freedom

third of the length of the corresponding sides from their nearest end. The co-ordinates of the nodes 13, 14, 15 and 16 are (1/2, 1/4, 1/4), (1/4, 1/2, 1/4), (1/4, 1/4, 1/2) and (1/3, 1/3, 1/3) respectively. The degrees of freedom at nodes 1 to 12, (except 3, 7 and 11) are u , v , w , θ_x and θ_y . It is only w at nodes 3, 7, 11, 13, 14 and 15. The centroidal node (16) has u , v , θ_x and θ_y as degrees of freedom.

The transverse displacement (w), in-plane displacements (u and v) and rotations of the normal (θ_x and θ_y) have been taken as independent field variables, which are as follows

$$u = [P_2]\{\chi\} \quad (1a)$$

$$v = [P_2]\{\beta\} \quad (1b)$$

$$w = [P_1]\{\gamma\} \quad (1c)$$

$$\theta_x = [P_2]\{\mu\} \quad (1d)$$

and
$$\theta_y = [P_2]\{\lambda\} \quad (1e)$$

where

$$[P_2] = [L_1^3 \ L_2^3 \ L_3^3 \ L_1^2L_2 \ L_2^2L_1 \ L_2^2L_3 \ L_3^2L_2 \ L_3^2L_1 \ L_1^2L_3 \ L_1L_2L_3],$$

$$[P_1] = [L_1^4 \ L_2^4 \ L_3^4 \ L_1^3L_2 \ L_2^3L_1 \ L_2^3L_3 \ L_3^3L_2 \ L_3^3L_1 \ L_1^3L_3 \ L_1^2L_2^2 \ L_2^2L_3^2 \ L_3^2L_1^2, \\ L_1^2L_2L_3 \ L_1L_2^2L_3 \ L_1L_2L_3^2],$$

$$\{\chi\} = [\alpha_1 \ \alpha_2 \ \alpha_3 \ \alpha_4 \ \alpha_5 \ \alpha_6 \ \alpha_7 \ \alpha_8 \ \alpha_9 \ \alpha_{10}]^T,$$

$$\{\beta\} = [\alpha_{11} \ \alpha_{12} \ \alpha_{13} \ \alpha_{14} \ \alpha_{15} \ \alpha_{16} \ \alpha_{17} \ \alpha_{18} \ \alpha_{19} \ \alpha_{20}]^T,$$

$$\{\gamma\} = [\alpha_{21} \ \alpha_{22} \ \alpha_{23} \ \alpha_{24} \ \alpha_{25} \ \alpha_{26} \ \alpha_{27} \ \alpha_{28} \ \alpha_{29} \ \alpha_{30} \ \alpha_{31} \ \alpha_{32} \ \alpha_{33} \ \alpha_{34} \ \alpha_{35}]^T,$$

$$\{\mu\} = [\alpha_{36} \ \alpha_{37} \ \alpha_{38} \ \alpha_{39} \ \alpha_{40} \ \alpha_{41} \ \alpha_{42} \ \alpha_{43} \ \alpha_{44} \ \alpha_{45}]^T,$$

and
$$\{\lambda\} = [\alpha_{46} \ \alpha_{47} \ \alpha_{48} \ \alpha_{49} \ \alpha_{50} \ \alpha_{51} \ \alpha_{52} \ \alpha_{53} \ \alpha_{54} \ \alpha_{55}]^T.$$

Now the above equations may be substituted appropriately at the different nodes with corresponding values of L_i of the nodes, which will give the relationship between the unknown coefficients of the above polynomials in Eqs. (1a-1e) and the nodal degrees of freedom as

$$\{\delta_e\} = [A]\{\alpha\} \quad \text{or} \quad \{\alpha\} = [A]^{-1}\{\delta_e\} \quad (2)$$

where

$$\{\alpha\} = \{\alpha_1 \ \alpha_2 \ \dots \ \alpha_{55}\}$$

$$\{\delta_e\}^T = [u_1v_1w_1\theta_{x1}\theta_{y1} \ u_2v_2w_2\theta_{x2}\theta_{y2} \ w_3 \ u_4v_4w_4\theta_{x4}\theta_{y4} \ u_5v_5w_5\theta_{x5}\theta_{y5}]$$

$$u_6 v_6 w_6 \theta_{x6} \theta_{y6} \quad w_7 \quad u_8 v_8 w_8 \theta_{x8} \theta_{y8} \quad u_9 v_9 w_9 \theta_{x9} \theta_{y9}$$

$$u_{10} v_{10} w_{10} \theta_{x10} \theta_{y10} \quad w_{11} \quad u_{12} v_{12} w_{12} \theta_{x12} \theta_{y12} \quad w_{13} \quad w_{14} \quad w_{15} \quad u_{16} v_{16} w_{16} \theta_{x16} \theta_{y16}]$$

and the matrix $[A]$ having an order of 55×55 contains the coordinates of the different nodes.

As the rotations of the normal θ_x and θ_y are independent field variables and they are not derivatives of w , the effect of shear deformation can be easily incorporated as follows

$$\begin{Bmatrix} \phi_x \\ \phi_y \end{Bmatrix} = \begin{Bmatrix} \theta_x - \partial w / \partial x \\ \theta_y - \partial w / \partial y \end{Bmatrix} \quad (3)$$

where ϕ_x and ϕ_y are the average shear strain over the entire plate thickness and θ_x and θ_y are the total rotations of the normal.

Now the generalized stress strain relationship of a plate may be written as

$$\{\sigma\} = [D]\{\varepsilon\} \quad (4)$$

In the above equation, the generalized stress vector $\{\sigma\}$ is

$$\{\sigma\}^T = [N_x \quad N_y \quad N_{xy} \quad M_x \quad M_y \quad M_{xy} \quad Q_x \quad Q_y] \quad (5)$$

and the generalized strain vector $\{\varepsilon\}$ in terms of displacement fields is

$$\{\varepsilon\} = \begin{Bmatrix} \partial u / \partial x \\ \partial v / \partial y \\ \partial u / \partial y + \partial v / \partial x \\ -\partial \theta_x / \partial x \\ -\partial \theta_y / \partial y \\ -\partial \theta_x / \partial y - \partial \theta_y / \partial x \\ -\theta_x + \partial w / \partial x \\ -\theta_y + \partial w / \partial y \end{Bmatrix} \quad (6)$$

Now, the field variables as defined in Eqs. (1a-1e) may be substituted in the generalized strain vector $\{\varepsilon\}$ as expressed in Eq. (6), which leads to

$$\{\varepsilon\} = [C]\{\alpha\} \quad (7)$$

where the matrix $[C]$ having an order of 5×55 contains L_i conform to Eqs. (1a-1c) and their derivatives with respect to x and y . Substituting Eq. (2) in Eq. (7), the generalized strain vector $\{\varepsilon\}$ may be expressed as

$$\{\boldsymbol{\varepsilon}\} = [B]\{\boldsymbol{\delta}_e\} \quad (8)$$

where $[B] = [C][A]^{-1}$.

The rigidity matrix $[D]$ constitutes of the contributions of its individual orthotropic layers oriented in different directions. Using the material properties and fiber orientations of these layers, it can be easily obtained following the usual steps available in any standard text on mechanics of fiber reinforced laminated composites. The rigidity matrix can be expressed as

$$[D] = \begin{bmatrix} A_{11} & A_{12} & A_{16} & B_{11} & B_{12} & B_{16} & 0 & 0 \\ A_{12} & A_{22} & A_{26} & B_{12} & B_{22} & B_{26} & 0 & 0 \\ A_{16} & A_{26} & A_{66} & B_{16} & B_{26} & B_{66} & 0 & 0 \\ B_{11} & B_{12} & B_{16} & D_{11} & D_{12} & D_{16} & 0 & 0 \\ B_{12} & B_{22} & B_{26} & D_{12} & D_{22} & D_{26} & 0 & 0 \\ B_{16} & B_{26} & B_{66} & D_{16} & D_{26} & D_{66} & 0 & 0 \\ 0 & 0 & 0 & 0 & 0 & 0 & A_{55} & A_{54} \\ 0 & 0 & 0 & 0 & 0 & 0 & A_{45} & A_{44} \end{bmatrix}$$

Once the matrices $[B]$ and $[D]$ are obtained, the element stiffness matrix $[K_e]$ can be easily derived with the help of Virtual work technique and it may be expressed as

$$[K_e] = \int_A [B]^T [D] [B] dx dy \quad (9)$$

In a similar manner, the consistent mass matrix of an element can be derived with the help of the Eqs. (1) and (2) and it may be expressed as

$$[M_e] = [A]^{-T} \rho h \int_A \left(\begin{array}{c} [P_u]^T [P_u] + [P_v]^T [P_v] + [P_w]^T [P_w] + \frac{h^2}{12} [P_{\theta_x}]^T [P_{\theta_x}] \\ + \frac{h^2}{12} [P_{\theta_y}]^T [P_{\theta_y}] \end{array} \right) dx dy [A]^{-1} \quad (10)$$

where,

$$\begin{aligned} [P_u] &= [[P_2]:[0]:[0]:[0]:[0]], \\ [P_v] &= [[0]:[P_2]:[0]:[0]:[0]], \\ [P_w] &= [[0]:[0]:[P_1]:[0]:[0]], \\ [P_{\theta_x}] &= [[0]:[0]:[0]:[P_2]:[0]] \\ [P_{\theta_y}] &= [[0]:[0]:[0]:[0]:[P_2]]. \end{aligned}$$

The first three terms of the mass matrix in Eq. (10) are associated with movement of mass along u , v and w directions respectively. The last two terms are associated with rotary inertia and their contribution becomes significant in the problem of thick plates. The integration in the above Eqs. (9) and (10) has been carried out numerically following Gauss quadrature technique.

Though the consistent mass matrix presented in Eq. (10) includes all the contributions including rotary inertia, it can not be used directly in the present analysis. In this consistent mass matrix the degrees of freedom at the internal nodes (which contains significant amount of mass) can not be eliminated but it is desired to eliminate these quantities for the improvement of computational elegance. This problem has been overcome by using lumped mass matrix $[M_l]$. The present lump mass matrix has been formed with the help of consistent mass matrix presented in Eq. (10). In this context two different mass lumping schemes have been recommended which are as follows.

In the first lumping scheme, the mass of an element m_e has been distributed at w of its external twelve nodes where the ratio of distribution is dependent on the corresponding diagonal masses of the consistent mass matrix $[M_e]$ presented in Eq. (10). This lumping scheme has been defined as LS12 and it is as follows

$$m_{ii}^{wl} = \frac{m_{ii}}{\sum m_{ii}} m_e \quad (i = 3, 8, 11, 14, 19, 24, 27, 30, 35, 40, 43, 46)$$

where m_{ii}^{wl} are the i th diagonal elements corresponding to w of the proposed lumped mass matrix, m_{ii} is the i th diagonal element of the consistent mass matrix $[M_e]$ and m_e is the mass of the element. The concept is similar to that of Hinton *et al.* (1976).

In the second lumping scheme, the effect of in-plane as well as rotary inertia have been taken into account. In this lumping scheme the external nine nodes containing the degrees of freedom of u , v , w , θ_x and θ_y have been considered. Similar technique has been followed to get it at the external nodes as follows

$$m_{ii}^{ul} = \frac{m_{ii}}{\sum m_{ii}} m_e \quad (i = 1, 6, 12, 17, 22, 28, 33, 38, 44)$$

$$m_{ii}^{vl} = \frac{m_{ii}}{\sum m_{ii}} m_e \quad (i = 2, 7, 13, 18, 23, 29, 34, 39, 45)$$

$$m_{ii}^{wl} = \frac{m_{ii}}{\sum m_{ii}} m_e \quad (i = 3, 8, 14, 19, 24, 30, 35, 40, 46)$$

$$m_{ii}^{\theta xl} = \frac{h^2}{12} \frac{m_{ii}}{\sum m_{ii}} m_e \quad (i = 4, 9, 15, 20, 25, 31, 36, 41, 47)$$

$$\text{and } m_{ii}^{\theta yl} = \frac{h^2}{12} \frac{m_{ii}}{\sum m_{ii}} m_e \quad (i = 5, 10, 16, 21, 26, 32, 37, 42, 48)$$

where the use of factor $(h^2/12)$ can be justified with the expression of the consistent mass matrix as presented in Eq. (10). This lumping scheme has been defined as LS9RI. In this way the lumped mass matrix (LS12 or LS9RI) obtained has zero masses at the internal nodes and it contains only diagonal

evaluated for all the elements and they have been assembled together to form the overall stiffness $[K]$ and mass matrix $[M]$ respectively. The storage of $[K]$ and $[M]$ has been done in single array following skyline storage technique with proper care for the different degrees of freedom at the different nodes. Once $[K]$ and $[M]$ are obtained, the equation of motion of the plate may be expressed as

$$[K] = \omega^2 [M] \quad (11)$$

After incorporating the boundary conditions in the above equation it has been solved by simultaneous iterative technique of Corr and Jennings (1976) to get frequency ω for first few modes.

3. Numerical examples

In order to demonstrate the accuracy and applicability of the present element, formulation and two different mass lumping (LS12 and LS9RI) schemes, few examples of isotropic trapezoidal plate and square composite laminate have been presented and compared with published results. To the best of the author's knowledge as there is no suitable published results for laminated composite trapezoidal plate, the solutions obtained for composite trapezoidal plate by the proposed element have been presented as new results. Unless otherwise mentioned the following material property and boundary conditions have been used for composite plate:

$$E_1 = 40 E_2, G_{12} = G_{13} = 0.6 E_2, G_{23} = 0.5 E_2, \nu_{12} = 0.25 \text{ and } \nu_{12} = \nu_{21}$$

Simply supported: $u_t = w = \theta_t = 0$

Clamped: $u_t = u_n = w = \theta_t = \theta_n = 0$

The degrees of freedom at the inclined boundary edges have been transformed into local axis system.

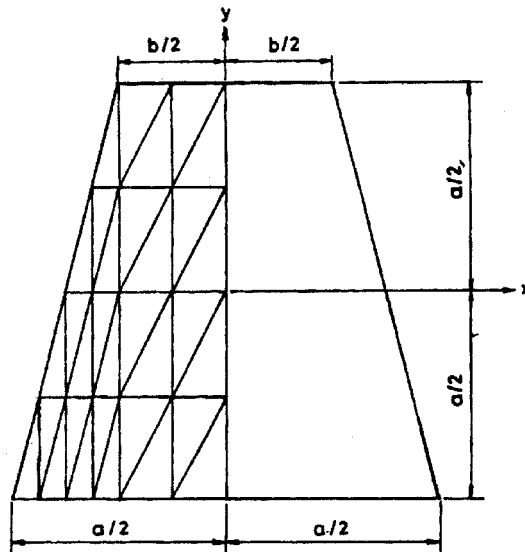


Fig. 2 A trapezoidal plate with mesh size: $(4 + 2) \times 4$

Table 1 First two non-dimensional frequency parameter $[(\alpha\alpha^2/2\pi)(\rho h/D)^{1/2}]$ of a simply-supported trapezoidal plate

b/a	Sources	For h/a = 0.01		For h/a = 0.1		For h/a = 0.2	
		Mode No.		Mode No.		Mode No.	
		1	2	1	2	1	2
4/5	LS12* (5+3)×5 [#]	3.511	8.227	3.279	7.476	2.952	6.277
	LS12 (7+3)×7	3.510	8.224	3.278	7.478	2.952	6.288
	LS12 (8+2)×8	3.510	8.223	3.278	7.479	2.953	6.291
	LS9RI** (5+3)×5	3.512	8.227	3.258	7.382	2.893	6.102
	LS9RI (7+3)×7	3.511	8.224	3.257	7.382	2.893	6.105
	LS9RI (8+2)×8	3.510	8.224	3.257	7.382	2.894	6.107
	Liew and Lam (1991)	3.52	8.24				
	% change***	0.0	0.0	0.645	1.314	2.039	3.013
3/5	LS12 (6+2)×6	4.070	8.882	3.785	7.985	3.378	6.645
	LS12 (6+3)×6	4.068	8.877	3.783	7.986	3.378	6.653
	LS12 (7+3)×7	4.067	8.875	3.782	7.987	3.378	6.657
	LS9RI (6+2)×6	4.073	8.886	3.758	7.881	3.306	6.450
	LS9RI (6+3)×6	4.068	8.878	3.755	7.877	3.304	6.452
	LS9RI (7+3)×7	4.067	8.876	3.755	7.877	3.307	6.452
	Liew and Lam (1991)	4.08	8.91				
	% change	0.0	0.0	0.719	1.396	2.147	3.177
2/5	LS12 (7+1)×7	4.900	10.15	4.540	8.993	4.002	7.363
	LS12 (8+1)×8	4.899	10.15	4.541	8.995	4.003	7.370
	LS12 (9+1)×9	4.898	10.15	4.541	8.996	4.003	7.374
	LS9RI (7+1)×7	4.911	10.18	4.511	8.879	3.914	7.150
	LS9RI (8+1)×8	4.903	10.17	4.511	8.881	3.915	7.155
	LS9RI (9+1)×9	4.900	10.17	4.511	8.882	3.915	7.157
	Liew and Lam (1991)	4.90	10.24				
	% change	0.04	0.197	0.665	1.283	2.248	3.032
1/5	LS12 (7+1)×7	5.992	12.64	5.529	11.06	4.792	8.809
	LS12 (8+1)×8	5.992	12.64	5.530	11.07	4.793	8.817
	LS12 (9+1)×9	5.992	12.64	5.530	11.07	4.794	8.823
	LS9RI (7+1)×7	5.991	12.63	5.474	10.87	4.665	8.481
	LS9RI (8+1)×8	5.992	12.63	5.474	10.88	4.666	8.484
	LS9RI (9+1)×9	5.992	12.63	5.475	10.88	4.667	8.486
	Liew and Lam (1991)	6.01	12.68				
	% change	0.0	0.08	1.004	1.746	2.72	3.97

*Present solutions considering lumping scheme LS12.

**Present solutions considering lumping scheme LS9RI.

#Mesh divisions.

***Percentage change of results due to lumping scheme LS9RI with respect to LS12

Table 2 Non-dimensional fundamental frequency parameter $[(\omega a^2)(\rho/E_2 h)^{1/2}]$ of a square laminate with different boundary conditions and ply orientations

Boundary conditions	h/a	Sources	For 0/90	For 0/90/0/90/0/90/0/90/0/90	For 45/-45	For 0/90/0/90
SSSS	0.01	LS12 (4×8)	11.304	18.613	15.018	17.278
		LS9RI (4×8)	11.299	18.608	15.015	17.277
		Reddy (1989)	11.300	18.610	14.863	17.278
		% change	0.044	0.027	0.02	0.006
	0.1	LS12 (4×8)	10.578	15.830	13.228	14.987
		LS9RI (4×8)	10.487	15.777	13.105	14.923
		Reddy (1989)	10.568	15.770	13.044	14.846
		% change	0.868	0.336	0.939	0.429
	0.2	LS12 (4×8)	9.0252	11.679		
		LS9RI (4×8)	8.8594	11.636		
		Reddy & Khdeir (1989)	8.833	11.644		
		% change	1.871	0.369		
CCSS	0.1	LS12 (4×8)	15.266	20.493		
		LS9RI (4×8)	15.165	20.455		
		Reddy & Khdeir (1989)	15.152	20.471		
		% change	0.666	0.1858		
	0.2	LS12 (4×8)	11.032	12.930		
		LS9RI (4×8)	10.908	12.904		
		Reddy & Khdeir (1989)	10.897	12.928		
		% change	1.137	0.201		
SSFC	0.1	LS12 (4×8)	7.7896	11.882		
		LS9RI (4×8)	7.7340	11.839		
		Reddy & Khdeir (1989)	7.741	11.862		
		% change	0.719	0.3632		
	0.2	LS12 (4×8)	6.7486	8.9447		
		LS9RI (4×8)	6.6438	8.9044		
		Reddy & Khdeir (1989)	6.638	8.919		
		% change	1.577	0.4526		
CFFF	0.01	LS12 (4×8)	2.6049			
		LS9RI (4×8)	2.6038			
		Reddy & Khdeir (1989)	2.6103			
		% change	0.042			
	0.1	LS12 (4×8)	2.5357			
		LS9RI (4×8)	2.5287			
		Reddy & Khdeir (1989)	2.5334			
		% change	0.277			

3.1. Isotropic trapezoidal plate

A simply supported isotropic trapezoidal plate as shown in Fig. 2 has been analyzed. The study has been done for three different thickness ratios ($h/a = 0.01, 0.1$ and 0.2). Utilizing symmetry in the structure, the analysis has been carried out by modeling half of the plate with different mesh divisions as shown in Fig. 2. The mesh division has been defined as $(m + n) \times m$, where m is the number of divisions of the triangular part in both the directions and n is the number of divisions for the rectangular portion along x direction. Both the lumping schemes (LS12 and LS9RI) have been used. The first two natural frequencies obtained have been presented with the analytical solution of Liew and Lam (1991) in Table 1. Liew and Lam (1991) used a computationally efficient Rayleigh-Ritz approach for analysis of the problem. In this example only w is restrained.

Table 3 First two non-dimensional frequency parameter $[(\omega a^2)(\rho/E_2h)^{1/2}]$ of a simply supported four layer symmetric (0/90/90/0) trapezoidal composite laminate

b/a	Sources	For $h/a = 0.01$		For $h/a = 0.1$		For $h/a = 0.2$	
		Mode No.		Mode No.		Mode No.	
		1	2	1	2	1	2
4/5	LS12 (6+1)×2	22.783	38.658	17.435	28.752	12.030	19.791
	LS12 (7+1)×2	22.782	38.657	17.439	28.770	12.038	19.828
	LS12 (8+1)×2	22.782	38.656	17.442	28.780	12.045	19.856
	LS9RI (6+1)×2	22.784	38.671	17.387	28.598	11.971	19.729
	LS9RI (7+1)×2	22.783	38.669	17.389	28.609	11.977	19.778
	LS9RI (8+1)×2	22.783	38.668	17.391	28.617	11.970	19.796
3/5	LS12 (6+1)×2	28.464	43.310	20.399	31.444	13.543	20.998
	LS12 (7+1)×2	28.443	43.291	20.403	31.460	13.552	21.032
	LS12 (8+1)×2	28.440	43.289	20.407	31.473	13.559	21.058
	LS9RI (6+1)×2	28.482	43.332	20.343	31.278	13.480	20.924
	LS9RI (7+1)×2	28.455	43.312	20.346	31.289	13.487	20.948
	LS9RI (8+1)×2	28.448	43.299	20.349	31.298	13.492	20.966
2/5	LS12 (8+1)×1	35.442	57.629	23.924	36.470	15.471	23.131
	LS12 (9+1)×1	35.412	57.629	23.932	36.501	15.480	23.162
	LS12 (10+1)×1	35.317	57.629	23.939	36.525	15.487	23.186
	LS9RI (8+1)×1	35.376	57.483	23.895	36.412	15.425	23.093
	LS9RI (9+1)×1	35.322	57.425	23.902	36.435	15.434	23.123
	LS9RI (10+1)×1	35.287	57.387	23.907	36.453	15.441	23.146
1/5	LS12 (8+1)×1	43.241	76.025	27.597	44.417	17.617	26.899
	LS12 (9+1)×1	43.122	76.025	27.606	44.454	17.626	26.931
	LS12 (10+1)×1	43.045	75.811	27.613	44.481	17.632	26.955
	LS9RI (8+1)×1	43.130	75.923	27.489	44.233	17.523	26.793
	LS9RI (9+1)×1	43.052	75.839	27.496	44.261	17.532	26.826
	LS9RI (10+1)×1	42.999	75.783	27.502	44.282	17.539	26.850

Table 4 First and second non-dimensional frequency parameter $[(\omega a^2)(\rho/E_2h)^{1/2}]$ of a clamped trapezoidal composite laminate

b/a	h/a	Sources	For 0/90		For 0/90/0		For 0/90/90/0	
			Mode No.		Mode No.		Mode No.	
			1	2	1	2	1	2
4/5	0.01	LS12 (8+2)×8	27.094	51.409	49.176	58.320	49.180	65.114
		LS9RI (8+2)×8	27.086	51.384	49.169	58.302	49.172	65.094
	0.1	LS12 (8+2)×8	20.609	34.188	23.574	31.691	24.732	36.189
		LS9RI (8+2)×8	20.517	33.952	23.540	31.518	24.723	36.127
	0.2	LS12 (8+2)×8	13.675	21.126	13.803	19.880	14.459	21.454
		LS9RI (8+2)×8	13.675	21.126	13.803	19.880	14.459	21.454
3/5	0.01	LS12 (8+2)×8	31.853	55.211	57.248	72.398	58.632	78.028
		LS9RI (8+2)×8	31.852	55.202	57.247	72.394	58.632	78.026
	0.1	LS12 (8+2)×8	23.198	36.269	26.421	34.620	27.532	38.699
		LS9RI (8+2)×8	23.101	36.013	26.384	34.432	27.525	38.625
	0.2	LS12 (8+2)×8	14.993	22.230	15.180	21.126	15.764	22.588
		LS9RI (8+2)×8	14.960	22.072	15.145	20.949	15.763	22.534
2/5	0.01	LS12 (9+1)×9	38.903	64.338	65.477	89.118	68.728	98.302
		LS9RI (9+1)×9	38.903	64.336	65.477	89.117	68.728	98.302
	0.1	LS12 (9+1)×9	26.689	40.102	29.629	39.252	30.955	42.852
		LS9RI (9+1)×9	26.640	49.940	29.627	39.152	30.955	42.850
	0.2	LS12 (9+1)×9	16.730	24.096	16.894	23.161	17.451	24.462
		LS9RI (9+1)×9	16.730	24.018	16.890	23.041	17.451	24.460
1/5	0.01	LS12 (9+1)×9	47.269	82.257	73.652	106.67	79.019	121.07
		LS9RI (9+1)×9	47.269	82.255	73.652	106.67	79.019	121.07
	0.1	LS12 (9+1)×9	30.764	46.893	32.991	45.759	34.768	49.561
		LS9RI (9+1)×9	30.623	46.555	32.900	45.560	34.739	49.439
	0.2	LS12 (9+1)×9	18.807	27.488	18.849	26.542	19.462	27.815
		LS9RI (9+1)×9	18.759	27.305	18.789	26.292	19.456	27.759

3.2. Laminated square plate

In this example a square laminate having different boundary conditions, ply-angle orientations and thickness ratios has been analyzed. The fundamental frequency obtained by the proposed element has been presented in Table 2 with the analytical solutions of Reddy (1989) and Reddy and Khdeir (1989).

In the above two examples, the results obtained by the present element have close agreement with the published analytical solutions. From the Tables it is seen that the rotary inertia has significant effect for thick plate. Therefore, LS9RI is recommended for both thick and thin plates and LS12 is recommended for thin plates.

3.3. Symmetric and anti-symmetric cross-ply trapezoidal plate

A simply supported symmetric cross ply ($0^0/90^0/90^0/0^0$) trapezoidal laminate (Fig. 2) has been

Table 5 First and second non-dimensional frequency parameter $[(\omega a^2)(\rho/E_2h)^{1/2}]$ of a simply supported two and ten layer (45/-45/45/-45---) trapezoidal composite laminate

b/a	N.N	Sources	For h/a = 0.01		For h/a = 0.1		For h/a = 0.2	
			Mode No.		Mode No.		Mode No.	
			1	2	1	2	1	2
4/5	2	LS12 (8+2)×8	18.032	41.369	15.384	30.811	11.742	20.413
		LS9RI (8+2)×8	18.031	41.369	15.276	30.496	11.632	19.882
	10	LS12 (8+2)×8	28.826	62.147	21.147	37.554	13.812	22.130
		LS9RI (8+2)×8	28.826	62.146	21.125	37.553	13.812	20.893
3/5	2	LS12 (8+2)×8	22.072	45.506	17.442	33.100	12.967	21.629
		LS9RI (8+2)×8	22.071	45.503	17.302	32.666	12.826	21.233
	10	LS12 (8+2)×8	34.369	68.891	23.412	40.037	15.003	23.340
		LS9RI (8+2)×8	34.367	68.887	23.384	40.029	15.000	23.330
2/5	2	LS12 (9+1)×9	27.732	54.395	20.113	37.017	14.507	23.565
		LS9RI (9+1)×9	27.731	54.390	19.945	36.717	14.347	23.385
	10	LS12 (9+1)×9	42.501	80.412	26.348	43.769	16.553	25.125
		LS9RI (9+1)×9	42.500	80.400	26.346	43.762	16.550	25.120
1/5	2	LS12 (9+1)×9	34.446	69.050	23.241	42.948	16.426	26.703
		LS9RI (9+1)×9	34.451	69.087	22.972	42.538	16.188	26.416
	10	LS12 (9+1)×9	52.705	99.358	30.080	49.751	18.594	28.288
		LS9RI (9+1)×9	52.729	99.420	30.014	49.717	18.573	28.270

N.N represent number of layer.

analyzed with different b/a and thickness ratios (h/a). Similar to the previous example, the half of the plate has been analyzed and two mass lumping schemes have been used. The first two non-dimensional frequencies obtained by the present element have been given in Table 3. Results have been presented with different mesh divisions to show the convergence of the element. In this analysis all degrees of freedom have been restrained except θ_n .

A clamped trapezoidal laminate with thickness ratio h/a = 0.01, 0.1 and 0.2 has been analyzed and the first two non-dimensional frequencies has been presented in Table 4. The analysis has been performed considering ply orientations $0^0/90^0$, $0^0/90^0/0^0$ and $0^0/90^0/90^0/0^0$.

3.4. Anti-symmetric angle ply trapezoidal laminate

First a simply supported two and ten layer (45⁰/-45⁰/45⁰/-45⁰-----) trapezoidal laminate has been analyzed with different b/a and h/a ratios. The analysis has been performed considering both the mass lumping schemes and the results have been presented in Table 5.

Next an anti-symmetric two layer trapezoidal laminate with different ply angles (30⁰/-30⁰, 45⁰/-45⁰ and 60⁰/-60⁰) has been analyzed. The two inclined edges of the laminate are simply supported and other two parallel edges are clamped. The first two non-dimensional frequencies obtained by the proposed element have been given in Table 6.

Table 6 First and second non-dimensional frequency parameter $[(\omega a^2)(\rho/E_2h)^{1/2}]$ of a two layer angle ply trapezoidal composite laminate with two inclined edges are simply supported and other two edges are clamped

<i>b/a</i>	<i>h/a</i>	Sources	30/-30		45/-45		60/-60	
			Mode No.		Mode No.		Mode No.	
			1	2	1	2	1	2
4/5	0.01	LS12 (8+2)×8	23.247	44.520	26.136	51.543	27.058	61.832
		LS9RI (8+2)×8	23.245	44.515	26.134	51.540	27.056	61.828
	0.1	LS12 (8+2)×8	17.856	31.103	19.050	34.376	18.811	36.564
		LS9RI (8+2)×8	17.780	30.904	18.983	34.142	18.723	36.343
	0.2	LS12 (8+2)×8	12.643	20.175	12.902	21.429	12.401	21.933
		LS9RI (8+2)×8	12.580	20.039	12.855	21.356	12.317	21.845
3/5	0.01	LS12 (8+2)×8	26.714	49.746	29.819	56.068	29.633	64.592
		LS9RI (8+2)×8	26.713	49.742	29.817	56.064	29.632	64.589
	0.1	LS12 (8+2)×8	19.791	33.547	20.832	36.462	20.092	37.870
		LS9RI (8+2)×8	19.684	33.345	20.761	36.213	19.992	37.610
	0.2	LS12 (8+2)×8	13.852	21.426	13.961	22.526	13.275	22.783
		LS9RI (8+2)×8	13.766	21.292	13.904	22.452	13.174	22.672
2/5	0.01	LS12 (9+1)×9	32.279	57.502	35.280	64.290	34.159	69.782
		LS9RI (9+1)×9	32.278	57.500	35.281	64.293	34.158	69.780
	0.1	LS12 (9+1)×9	22.580	37.103	23.207	39.776	22.039	40.152
		LS9RI (9+1)×9	22.468	36.946	23.157	39.653	21.966	39.950
	0.2	LS12 (9+1)×9	15.513	23.316	15.387	24.242	14.550	24.179
		LS9RI (9+1)×9	15.435	23.236	15.335	24.163	14.453	24.123
1/5	0.01	LS12 (9+1)×9	40.173	69.798	42.478	77.445	41.272	79.817
		LS9RI (9+1)×9	40.172	69.795	42.477	77.444	41.275	79.821
	0.1	LS12 (9+1)×9	26.362	42.852	26.352	45.105	24.886	44.648
		LS9RI (9+1)×9	26.166	42.469	26.190	44.843	24.719	44.300
	0.2	LS12 (9+1)×9	17.616	26.514	17.280	27.247	16.354	26.975
		LS9RI (9+1)×9	17.497	26.304	17.156	27.172	16.180	26.812

3.5. Isotropic and laminated composite plate with concentrated mass at the centre

Vibration of an isotropic rectangular plate, 0.71 m long, 0.42 m wide and 2.0 mm thick having a concentrated mass at the centre with self mass has been studied. The plate is simply supported at the two opposite smaller sides and clamped along the other two longer sides. The present results for different values of concentrated mass have been presented in Table 7 with those obtained by Ritz solution of Boay (1995). The material properties of the plate are:

$$E = 70.0 \text{ Gpa}, \nu = 0.3 \text{ and } \rho = 1770 \text{ kg/m}^3$$

A simply supported two layer cross ply square laminate having concentrated mass at the centre

Table 7 Fundamental frequency parameter $\omega/2\pi$ and $(\omega\alpha^2)(\rho/E_2h)^{1/2}$ for isotropic and two layer (0/90) cross ply square laminate respectively having a concentrated mass (M) at the centre

For isotropic plate				
M (kg)	Present analysis			Boay (1995)
	LS12 (3×4)	LS12 (4×6)	LS12 (5×6)	
0.5	38.78	38.73	38.72	38.83
1.0	29.52	29.49	29.48	29.54
1.48	24.92	24.89	24.87	24.96
1.98	21.84	21.80	21.79	21.88
3.0	17.99	17.94	17.93	18.03
For two layer cross ply laminate				
$M/\rho ha^2$	Sources	$h/a = 0.01$	$h/a = 0.1$	$h/a = 0.2$
0.5	LS12 (4×8)	5.4672	4.6163	3.3231
	LS9RI (4×8)	5.4669	4.6078	3.3165
	Dey	5.4700	4.6170	3.3235
1.0	LS12 (4×8)	4.1952	3.4384	2.4108
	LS9RI (4×8)	4.1951	3.4351	2.4085
	Dey	4.1960	3.4391	2.4112
2.0	LS12 (4×8)	3.1052	2.4965	1.7258
	LS9RI (4×8)	3.1052	2.4953	1.7250
	Dey	3.1053	2.4969	1.7260

with self mass has been analyzed considering two different mass lumping schemes. The analysis has been done considering different mass ratio $M/\rho ha^2$, where M is the concentrated mass and ρ is mass density, h is thickness and a is length of the square laminate respectively. The first two non-dimensional frequencies have been presented in Table 7 with those of Dey. Dey one of the co-researchers has analyzed the problem using a seven node triangular element with 16×16 mesh divisions.

The above two examples have been presented only to validate the proposed element, formulation and the mass lumping schemes. There is excellent agreement between the results.

Finally a simply supported two layer cross ply (0⁰/90⁰) trapezoidal laminate having concentrated mass at the centre with the self mass has been analyzed and presented in Table 8. In this example the following material properties are used:

$$E_1 = 25 E_2, G_{12} = G_{13} = 0.5E_2, G_{23} = 0.2 E_2, \nu_{12} = 0.25 \text{ and } \nu_{12} = \nu_{21}$$

4. Conclusions

A high precision shear deformable triangular element has been proposed and applied to free vibration analysis of laminated trapezoidal plate. First order shear deformation theory has been incorporated in the element formulation. The performance of the element has been tested through convergence test as

Table 8 First two non-dimensional frequency parameter $[(\omega\alpha^2)(\rho/E_2h)^{1/2}]$ of a simply supported two layer (0/90) trapezoidal laminate having a concentrated mass (M) at the centre

b/a	$M/\rho ha^2$	Sources	For $h/a = 0.01$		For $h/a = 0.1$		For $h/a = 0.2$		
			Mode No.		Mode No.		Mode No.		
			1	2	1	2	1	2	
4/5	0	LS12 (8+2)×8	11.239	27.668	10.061	22.242	8.2670	15.603	
		LS9RI (8+2)×8	11.239	27.667	9.9788	21.992	8.1383	13.934	
	0.5	LS12 (8+2)×8	6.3118	27.636	5.1457	18.162	3.6509	11.288	
		LS9RI (8+2)×8	6.3118	27.636	5.1354	18.067	3.6429	11.154	
	1.0	LS12 (8+2)×8	4.8372	27.625	3.8286	16.324	2.6486	11.027	
		LS9RI (8+2)×8	4.8372	27.625	3.8245	16.229	2.6457	10.888	
	2.0	LS12 (8+2)×8	3.3774	27.616	2.7780	16.917	1.8960	10.904	
		LS9RI (8+2)×8	3.3774	27.616	2.7765	16.817	1.8949	10.762	
	3/5	0	LS12 (8+2)×8	14.462	29.963	11.800	23.472	9.3726	16.380
			LS9RI (8+2)×8	14.461	29.963	11.696	23.187	9.2264	16.179
0.5		LS12 (8+2)×8	8.0009	29.655	5.8602	19.567	3.9752	12.280	
		LS9RI (8+2)×8	8.0010	29.654	5.8491	19.440	3.9679	12.123	
1.0		LS12 (8+2)×8	6.1044	29.570	4.3324	18.812	2.8720	12.047	
		LS9RI (8+2)×8	6.1044	29.570	4.3282	18.682	2.8694	11.886	
2.0		LS12 (8+2)×8	4.5011	29.509	3.1324	18.442	2.0517	11.937	
		LS9RI (8+2)×8	4.5011	29.509	3.1308	18.309	2.0508	11.774	
2/5		0	LS12 (9+1)×9	19.827	36.326	14.470	26.210	10.935	17.861
			LS9RI (9+1)×9	19.827	36.325	14.357	25.940	10.791	17.700
	0.5	LS12 (9+1)×9	10.937	32.506	7.2893	21.935	4.8665	14.215	
		LS9RI (9+1)×9	10.937	32.503	7.2770	21.762	4.8584	14.057	
	1.0	LS12 (9+1)×9	8.2989	31.976	5.3982	21.372	3.5361	13.977	
		LS9RI (9+1)×9	8.2989	31.974	5.3934	21.203	3.5332	13.814	
	2.0	LS12 (9+1)×9	6.0958	31.722	3.9068	21.080	2.5337	13.861	
		LS9RI (9+1)×9	6.0958	31.720	3.9050	21.913	2.5327	13.697	
	1/5	0	LS12 (9+1)×9	26.109	50.149	17.771	32.110	12.800	20.796
			LS9RI (9+1)×9	26.107	50.141	17.582	31.700	12.610	20.578
0.5		LS12 (9+1)×9	15.127	36.607	8.8739	23.207	5.5594	15.204	
		LS9RI (9+1)×9	15.126	36.604	8.8597	22.958	5.5530	14.987	
1.0		LS12 (9+1)×9	11.427	35.626	6.5131	22.731	4.0161	15.033	
		LS9RI (9+1)×9	11.428	35.628	6.5080	22.478	4.0139	14.811	
2.0		LS12 (9+1)×9	8.3623	35.131	4.6899	22.502	2.8692	14.952	
		LS9RI (9+1)×9	8.3624	35.133	4.6881	22.248	2.8684	14.729	

well as comparison of the present results with the available published results. Any numerical problem such as shear locking has not been encountered for thin plate. Two different mass lumping schemes have been recommended. In one of the mass lumping schemes rotary inertia has been included and it is seen that rotary inertia has significant effect for thick plate. The potential of the element and the concept of the present lumping schemes have been clearly reflected by the order of accuracy of the results in all the problems. In this investigation, a number of new results have been presented.

References

- Batoz, J. L. and Katili, I. (1992), "On a simple triangular Reissner/Mindlin plate element based on incompatible modes and discrete constraints", *Int. J. Num. Meth. Eng.*, **35**, 1603-1632.
- Boay, C. G. (1995), "Frequency analysis of rectangular isotropic plates carrying a concentrated mass", *Compt. Struct.* **56**(1), 39-48.
- Corr, R. B. and Jennings. A. (1976), "A simultaneous iteration algorithm for symmetric eigenvalue problems", *Int. J. Num. Meth. Eng.*, **10**, 647-663.
- Dey, P. Private communication.
- Gallagher, R. H. (1975), *Finite Element Analysis, Fundamentals*, Prentice-Hall, Englewood Cliffs, NJ.
- Hinton, E., Rock, T. and Zienkiewicz, O. C. (1976), "A note on mass lumping and related processes in the finite element method", *Earthquake Eng. and Struct. Dynamics*, **4**, 245-249.
- Liew, K. M. (1992), "Response of plates of arbitrary shape subjected to static loading", *J. Eng. Mech. ASCE*, **118**(9), 1783-1794.
- Liew, K. M. and Lam, K. Y. (1991), "A Rayleigh-Ritz approach to transverse vibration of isotropic and anisotropic trapezoidal plates using orthogonal plate functions", *Int. J. Solids Struct.* **27**(2), 189-203.
- Liew, K. M. and Lim, C. W. (1995), "Vibratory characteristics of general laminates, I: symmetric trapezoids", *J. Sound. Vibr.* **183**, 615-642.
- Lim, C. W., Liew, K. M. and Kitipornchai, S. (1996), "Vibration of arbitrarily laminated plates of general trapezoidal planform", *J. Acous. Soc. Am.* **100**, 3674-3685.
- Liew, K. M., Karunasena, W., Kitipornchai, S. and Chen, C. C. (1999), "Vibration of unsymmetrically laminated thick quadrilateral plates", *J. Acous. Soc. Am.* **105**, 1672-1681.
- Petrolito, J. (1989), "A modified ACM element for thick plate analysis", *Compt. Struct.*, **32**, 1303-1309.
- Reddy, J. N. (1989), "On refined computational modes of composite laminates", *Int. J. Num. Meth. Eng.*, **27**, 361-382.
- Reddy, J. N. and Khdeir, A. A. (1989), "Buckling and vibration of laminated composite plates using various plate theory", *AIAAJ*, **27**, 1808-1817.
- Sengupta, D. (1991), "Stress analysis of flat plates with shear using explicit stiffness matrix", *Int. J. Num. Meth. Eng.*, **32**, 1389-1409.
- Timoshenko, S. P. and Woinowsky-Krieger, S. (1959), *Theory of Plates and Shells*, McGraw-Hill, New York.
- Wanji, C. and Cheung, Y. K. (2000), "Refined quadrilateral element based on Mindlin/Reissner plate theory", *Int. J. Num. Meth. Eng.*, **47**, 605-627.
- Yuan, F. G. and Miller, R. E. (1989), "A cubic triangular finite element for flat plates with shear", *Int. J. Num. Meth. Eng.*, **28**, 109-126.
- Zhongnian Xu. (1992), "A thick-thin triangular plate element", *Int. J. Num. Meth. Eng.*, **33**, 963-973.
- Zienkiewicz, O. C. (1971), *The Finite Element Method in Engineering Science*, McGraw-Hill, New York.
- Zienkiewicz, O. C. and Taylor, R. L. (1988), *The Finite Element Method (two volumes)*, McGraw-Hill, New York.